The Astrophysical Journal, 611:L37–L40, 2004 August 10
© 2004. The American Astronomical Society. All rights reserved. Printed in U.S.A.

MIRA'S APPARENT SIZE VARIATIONS DUE TO A SURROUNDING SEMIOPAQUE H_2O LAYER

J. Weiner
Space Sciences Laboratory and Department of Physics, University of California at Berkeley, Grizzly Peak at Centennial Drive, Berkeley, CA 94720; johnw@ssl.berkeley.edu
Received 2004 May 21; accepted 2004 June 24; published 2004 July 12

ABSTRACT

The variations in Mira's apparent size across the near- and mid-infrared are explained in terms of a single H_2O shell surrounding the star. This simple model, consisting of a 2200 K H_2O shell of column density 7×10^{19} cm^{-2} and radius 30.3 mas surrounding a 2700 K star of radius 12.8 mas, successfully reproduces a wide variety of interferometric and photometric observations that have been made near maximum phase.

Subject headings: infrared: stars — stars: AGB and post-AGB — stars: atmospheres — stars: individual (*o* Ceti) — techniques: interferometric

1. INTRODUCTION

The apparent size of *o* Cet (Mira) has been measured by multiple instruments using interferometry and other high-resolution techniques at various wavelengths in the visible and infrared (Fig. 1). These diameters (obtained by modeling the star as a uniform intensity disk) are seen to vary by almost a factor of 3 across the near-infrared alone, and these variations are not primarily related to the stellar phase. At some wavelengths, differing apparent sizes were recorded because visibilities were measured at different resolutions[1] or at different position angles (Weiner et al. 2003; Quirrenbach et al. 1992), thus indicating a more complex (and possibly asymmetric) intensity distribution and a visibility curve substantially different from that of a simple disk. However, it has long been suggested that the gross variation of stellar size with wavelength can be understood only as the result of a molecular layer surrounding the star at radii sufficiently beyond the continuum photosphere (Perrin et al. 1999; Tej et al. 2003; Mennesson et al. 2002; Tuthill et al. 1999). In particular, Perrin et al. (2004) have fitted visibilities in several infrared bands to a model consisting of a star surrounded by a molecular shell with opacity adjusted for a best fit at each wavelength.

Unlike more static stars, Mira variables undergo significant pulsation that greatly redistributes and extends their atmospheres (Höfner et al. 1998). This extended atmosphere is relatively cooler than the inner photosphere and contains densities sufficient for molecules to form. The dynamical model atmosphere calculated by Woitke et al. (1999) predicts H_2O will form beyond $1.5R_*$ with a column density of about 10^{19} cm^{-2}. Tej et al. (2003) predict discrete shells of H_2O to form in the atmospheres of Mira variables with column densities as high as 10^{20} cm^{-2} and radii as large as $3R_*$ for some models near maximum luminosity.

Wallace & Hinkle (1996) identify individual H_2O lines in high-resolution *K*-band spectra of Mira but do not estimate the temperature or column density. Yamamura et al. (1999) obtain a fit to the spectra of *o* Cet between 2.5 and 4.7 μm by modeling the star as a 3000 K blackbody surrounded by a "hot" 2000 K H_2O shell at $2.0R_*$ having a column density of 3×10^{21} cm^{-2} and a "cool" 1400 K H_2O shell at $2.3R_*$ with a column density of 3×10^{20} cm^{-2}. SiO and CO_2 were also included in the fit to the spectra and are important for wavelengths greater than 4 μm. A cool H_2O shell somewhat like that of Yamamura et al. (1999) was observed by Weiner et al. (2003) using both high-resolution 11 μm spectra and narrowband interferometric visibilities on spectral lines. The shell was estimated to have a temperature of 1300 K, a radius of about $1.75R_*$, and a column density greater than $\sim 10^{19}$ cm^{-2}. No evidence of a hot 2000 K H_2O shell with greater density was noted in the spectra by Weiner et al. (2003).

In this Letter, we attempt to construct a cohesive model of Mira as a star surrounded by an H_2O layer that fits all relevant observations. Spectral and photometric studies measure the combined flux of the H_2O layer and the star, making a determination of both the temperature and the size of each difficult. On the other hand, interferometric studies are sensitive to apparent size but typically consist of averages over bandpasses wide enough to contain both spectral lines and continua. By simultaneously fitting both kinds of observations at various wavelengths, a more realistic picture of Mira's atmosphere is developed.

2. OBSERVATIONS OF MIRA COMPARED WITH THE H_2O SHELL MODEL

The model considered in this Letter consists of a spherical star of radius R_*, assumed to emit as an opaque blackbody of temperature T_*, surrounded by a region of zero opacity bounded by a thin spherical shell of H_2O gas of radius R_{H_2O} and column density N_c. The H_2O gas in the shell is further supposed to be populated in accordance with a single excitation temperature, T_{H_2O}. Since the 11 μm visibilities and photometry are affected by the presence of circumstellar dust, a well-resolved dust shell that contributes a fraction $A_{dust} = I_{dust}/(I_{dust} + I_{H_2O} + I_*)$ to the 11 μm flux is added to the model.[2] In general, this dust is cool enough to not contribute significant flux at shorter wavelengths, and Mennesson et al. (2002) discuss why such a dust shell does not affect the near-infrared visibilities or fluxes significantly. Thus, it is neglected for all observations below 5 μm. In theory, other molecules such as those considered by Jacob & Scholz (2002) may be present in Mira's circumstellar environment. However, their spectral lines are generally more localized than those of H_2O and do not play a critical role in affecting Mira's apparent size in the bandpasses considered below.

A list of the observations for which the model was optimized is given in Table 1. Since H_2O is the only molecule included

[1] The Infrared Optical Telescope Array (IOTA) recorded a range of uniform disk diameters for *o* Cet in the *L*' band (Mennesson et al. 2002). In addition, the *K*-band apparent size of *o* Cet reported in Tuthill et al. (1999) and measured at resolutions below 4×10^6 rad^{-1} differs from that reported by Mennesson et al. (2002), which was measured at a resolution of 8×10^6 rad^{-1}.

[2] The dust shell has the effect of scaling the 11 μm visibilities by the constant A_{dust} and increasing the 11 μm flux by A_{dust}^{-1}.

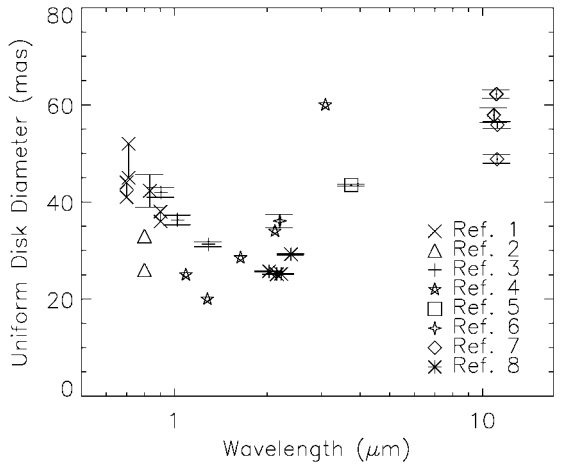

FIG. 1.—Various published uniform disk diameters of *o* Cet: (1) Haniff et al. 1995; (2) Quirrenbach et al. 1992; (3) Young et al. 1999; (4) Tuthill et al. 1999; (5) Mennesson et al. 2000; (6) Ridgway et al. 1992; (7) Weiner et al. 2003; (8) Perrin et al. 2004.

in this model, only observations at wavelengths greater than 1 μm were included.[3] The observations span many cycles but are all near maximum (between phases 0.81 and 0.21).[4] Hence, the description of the water shell obtained applies only near maximum luminosity. For modeling, all bandpasses were assumed to be Gaussian in shape with a FWHM given by the bandwidth listed. At every wavelength within each bandpass, the cross section, σ, of the H_2O gas was calculated using the line list of Partridge & Schwenke (1997), which was calculated from a semiempirical model of the H_2O molecule. The line positions are believed to be accurate to better than 0.1 cm^{-1}. A nominal line width of 8 km s^{-1} (FHWM) was chosen to correspond with observed line widths from the 11 μm spectra.

[3] TiO has been observed to affect the apparent sizes of cool stars in the visible (Quirrenbach et al. 2001).

[4] The apparent size of *o* Cet at 11 μm has been shown to depend on phase, indicating that the water shell, which is optically rather dense at this wavelength, changes size or density with stellar phase (Weiner et al. 2003).

The intensity distribution (as a function of angle, x) and at each wavelength is given by

$$I_\nu(x, \lambda) = \begin{cases} B_\nu(T_*)e^{-\tau(x,\lambda)} + B_\nu(T_{H_2O})(1 - e^{-\tau(x,\lambda)}), \\ \quad x < R_*, \\ B_\nu(T_{H_2O})(1 - e^{-2\tau(x,\lambda)}), \\ \quad R_* < x < R_{H_2O}, \end{cases} \quad (1)$$

where

$$B_\nu(T) = \frac{2hc\lambda^{-3}}{e^{h\nu/kT} - 1} \text{ and } \tau(x, \lambda) = \frac{\sigma(\lambda)N_c}{\sqrt{1 - x^2/R_{H_2O}^2}}.$$

The model fluxes were calculated by integrating the intensity distribution first over the image space and then over the bandpass. The model visibilities were calculated by taking the Hankel transform of the intensity distribution integrated over the bandpass. Since the four sets of visibility data from Tuthill et al. (1999) are known to have uncertain calibration, the visibility calibration for these sets was left free and optimized for a best fit (as was done in the original publication).

The "best-fitting" model was obtained by minimizing χ^2 with respect to the five-parameter model space.[5] The absolute minima of the χ^2 occurred at an H_2O shell temperature around 2500 K. Since H_2O dissociation was not included in the model and should occur around 2200 K (depending on the local density), we have adopted the best-fitting 2200 K model instead, which has a χ^2 only 7% larger than the absolute minimum. Both models visually fit the data equally well. The adopted best-fitting parameters are shown in Table 2. Although the line width was not fitted, some of the spectral lines do become saturated, and it is recognized that there is some dependence of the optimal column density on the chosen line width.

The visibility observations and the best-fitting model are

[5] Since it is recognized that this model will have deficiencies on a fine scale (from the presence of stellar hot spots or asymmetries, for instance), some of the error bars of the visibility measurements were increased so as to roughly fit all of the observations as opposed to fitting well only those with small statistical uncertainties.

TABLE 1
COMPILATION OF OBSERVATIONS TO BE COMPARED WITH THE MODEL

Wavelength (μm)	Bandwidth (FWHM, μm)	Observation	Phase	Instrument	Reference
1.24	0.0124	Visibilities	9.95	Keck	1
1.65	0.0165	Visibilities	9.95	Keck	1
2.26	0.0226	Visibilities	9.95	Keck	1
3.08	0.0308	Visibilities	9.95	Keck	1
2.03	0.10	Visibilities	13.01, 14.19–14.21	IOTA	2
2.15	0.10	Visibilities	13.01, 14.19–14.21	IOTA	2
2.22	0.10	Visibilities	13.01, 14.19–14.21	IOTA	2
2.39	0.10	Visibilities	13.01, 14.19–14.21	IOTA	2
3.79	0.54	Visibilities	13.10–13.13	IOTA	3
11.149	0.00207	Visibilities	13.08	ISI	4
1.25	0.3	Photometry[a]	0.81	ESO 1 m	5
1.6	0.4	Photometry[a]	0.81	ESO 1 m	5
2.2	0.6	Photometry[a]	0.81	ESO 1 m	5
3.6	1.0	Photometry[a]	0.81	ESO 1 m	5
4.8	0.6	Photometry[a]	0.81	ESO 1 m	5
11.149	0.00207	Photometry	0.99	UKIRT	6

[a] This photometry was calibrated using the zero fluxes of Moorwood & Salinari (1981).

REFERENCES.—(1) Tuthill et al. 1999; (2) Perrin et al. 2004; (3) Chagnon et al. 2002; (4) Weiner et al. 2003; (5) Fouqué et al. 1992; (6) Danchi et al. 1994; (7) Yamamura et al. 1999.

TABLE 2

BEST-FITTING H_2O SHELL MODEL PARAMETERS

Parameter	Value
R_*	12.78 mas
T_*	2701 K[a]
R_{H_2O}	30.32 mas
T_{H_2O}	2200 K
N_c	7.047×10^{19} cm^{-2}
A_{dust}	0.7214

[a] Since the photometry measurements involved in the fit were taken at phase 0.81, it is believed that the stellar temperature of 2701 K more closely describes this pre-maximum state and may be hotter at maximum.

shown in Figure 2. It is clear that the model reproduces the gross behavior of the visibilities including, most importantly, the factor of 3 change in apparent size between the wavelengths. It should be noted that the poorest fit to the visibilities occurs at 2.39 μm, which appears to require additional extrastellar opacity. The authors of this data (Perrin et al. 2004) suggest such a contribution from molecular carbon monoxide that is expected to be present but was not included in this study. Its spectral features are much more localized than those of H_2O.

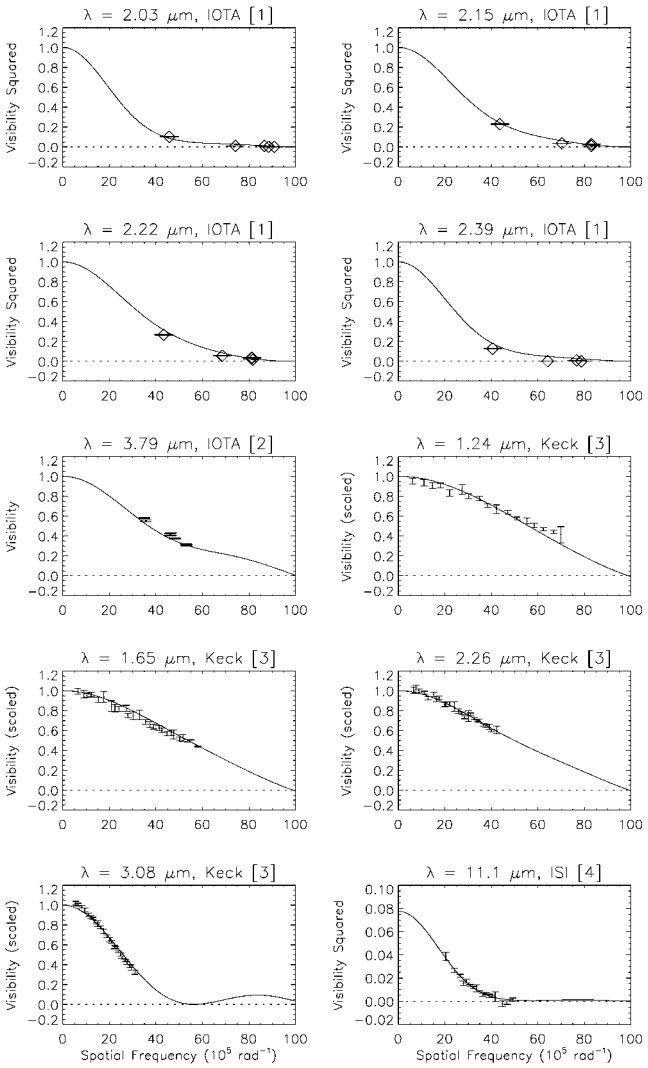

FIG. 2.—Infrared visibility observations and H_2O shell model fit: (1) Perrin et al. 2004; (2) Chagnon et al. 2002; (3) Tuthill et al. 1999; (4) Weiner et al. 2003.

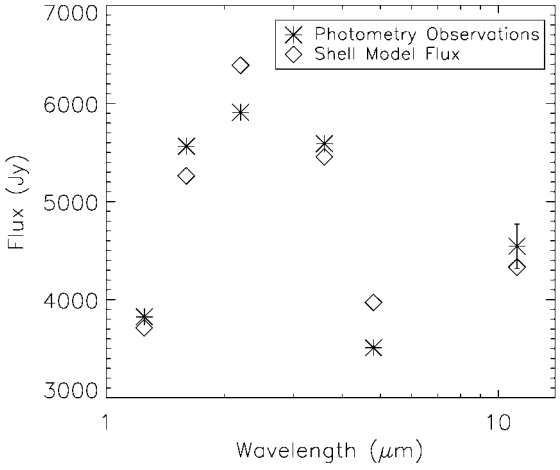

FIG. 3.—Infrared photometry and H_2O shell model fit.

The photometry data and the best-fitting model are shown in Figure 3. Since the visibilities are insensitive to proportional increases or decreases in the shell and stellar disk intensities, the photometry is the primary tool for determining the absolute intensities and, thus, the temperatures of the star and shell. Since the near-infrared photometry was recorded at phase 0.81 (rather than at maximum), the best-fitting stellar temperature of 2701 K probably describes this premaximum state. Thus, it is possible that the star will be hotter at maximum.

3. MID-INFRARED HIGH-RESOLUTION SPECTRA

High-resolution 11 μm spectra of *o* Cet were recorded at the Infrared Telescope Facility using the Texas Echelon Cross Echelle Spectrograph[6] for comparison with these H_2O shell models. These spectra (at five different dates) are displayed in Figure 4. The most prominent spectral lines can be readily identified as originating from a cool H_2O region located at a large radius and producing emission as reported in Weiner et al. (2003). A model of this "cool" shell (having an excitation temperature of 1200 K, a column density of 5×10^{19} cm^{-2}, and a radius 2.2 times larger than an

[6] The observations were carried out by J. Lacy and M. Richter, and a description of the instrument can be found in Lacy et al. (2002).

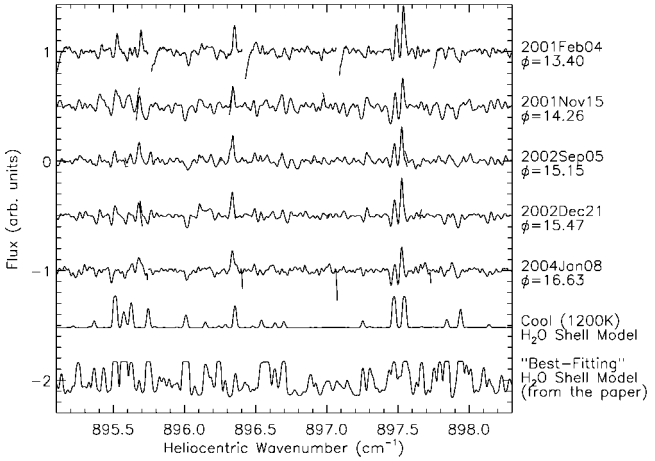

FIG. 4.—The 11 μm spectroscopy from various dates and model spectra. The "best-fitting" model is the one that best fits the visibility and photometry observations considered in the Letter and is described in Table 2.

opaque[7] 2200 K layer below it) is also displayed in Figure 4. Since the spectral lines in this cool shell are so sparse in frequency, the inclusion of this shell into the previous best-fitting model does not significantly affect the fits to either the visibilities or the fluxes. The observed spectral lines show some absorption at a wavenumber 11 km s^{-1} below the emission peak, indicating an infalling layer. This feature is not reproduced by the static cool shell model. A similar cool shell was also observed by Yamamura et al. (1999) in the near-infrared.

The best-fitting model spectra (corresponding to the parameters in Table 2) is also plotted in Figure 4. The most striking feature of this model spectra are the variations between opaque regions and mostly transparent regions. The flux is modeled to be about 35% lower in the lower opacity regions. However, the actual spectra show no signs of these fluctuations. In particular, the region between 896.7 and 897.2 cm^{-1} is especially flat in all of the observed spectra. Moreover, the best-fitting model is particularly sensitive to the choice of column density. Hence, flattening this spectra with increased H_2O opacity would ruin the fits to the near-infrared visibilities.

There are several possible explanations for this apparent contradiction. The simplest is that the velocity field of the 2200 K H_2O layer is quite turbulent and the model spectral lines should be broadened substantially. Furthermore, if the velocity field is turbulent on a large scale, the velocity dispersion will not be smooth but would contain many small fluctuations as are seen in the spectra. Another possibility is that the LTE thin shell model considered here is too simplistic to account for all of the observations. Perhaps a continuous H_2O distribution or a more accurate determination of the populations of the H_2O energy levels (in nonequilibrium) could find common ground between these observations.

4. CONCLUSIONS

H_2O as an opacity source in Mira's atmosphere has been suggested for some time. High spatial resolution data have been interpreted as molecular shells, spectral studies have modeled the structure of those H_2O regions, and theoretical models of H_2O's formation and effect on observations have been constructed. However, a single description of an H_2O shell that accounts for all available and relevent observations has not previously been presented.

By combining interferometry and photometry at multiple wavelengths, including those at which the H_2O layer is opaque, transparent, and, most critically, partially transparent, one can determine the three characteristic properties of this H_2O layer: temperature, radius, and column density. That such a simple model can account for the gross behavior of most observations, including the variations in apparent size, implies that this general picture is close to reality. The specific structure of the H_2O layer may well be different from that of a thin shell. In fact, an extended region of 2200 K H_2O from the stellar surface out to a radius of 33 mas having uniform density (and column density $\sim 7 \times 10^{19}$ cm^{-2}) also fits all of the observations included in this Letter. It is the outer edge of the H_2O that most determines its apparent size. Undoubtedly, other complications including a more complex radial distribution, other molecules, limb darkening, nonsphericity, and cycle-to-cycle variations are also present to varying degrees.

In spite of the uncertainties, some conclusions can be drawn about this H_2O layer (including its existence). As mentioned before, the column density is probably the most well-determined parameter. Changing it by as little as a factor of 2 would make it incompatible with near-infrared visibilities at the semitransparent wavelengths. The radii of the H_2O shell and the star are also quite well determined (to a few percent) since precise measurements of apparent size have been performed both at wavelengths at which the shell is opaque and at those where only the star is visible. However, the shell radius must be interpreted as the outer radius of the region of pronounced H_2O opacity rather than simply where all of the H_2O is located. The temperatures are the least precise of the five parameters in Table 2 (with uncertainty of a few hundred kelvin). Both are very dependent on the photometry and may change greatly with phase. In addition, it may be that a single H_2O excitation temperature is not realistic, either because the molecules are not in LTE or because the H_2O region has a temperature gradient. Finally, the smaller stellar size revealed by this interpretation is in much closer agreement with dynamical theories of fundamental-mode pulsation (Bowen 1988).

This work was supported in part by the National Science Foundation (AST 97-31625), the Office of Naval Research (N00014-89-J-1583), and the Gordon and Betty Moore Foundation. We are grateful to Matt Richter and John Lacy for their privately supplied mid-infrared spectrum of *o* Cet and to Guy Perrin, John Monnier, Peter Tuthill, and Jason Aufdenberg for their helpful discussions and advice.

[7] The plotted cool spectra involve an opaque 2200 K layer below them. This was done to isolate the effect of the cool shell. Of course, the 2200 K H_2O layer being described is not completely opaque, and its spectra is discussed in the following paragraph.

REFERENCES

Bowen, G. H. 1988, ApJ, 329, 299
Chagnon, G., et al. 2002, AJ, 124, 2821
Danchi, W. C., Bester, M., Degiacomi, C. G., Greenhill, L. J., & Townes, C. H. 1994, AJ, 107, 1469
Fouqué, P., Le Bertre, T., Epchtein, N., Guglielmo, F., & Kerschbaum, F. 1992, A&AS, 93, 151
Haniff, C. A., Scholz, M., & Tuthill, P. G. 1995, MNRAS, 276, 640
Höfner, S., Jørgensen, U. G., Loidl, R., & Aringer, B. 1998, A&A, 340, 497
Jacob, A. P., & Scholz, M. 2002, MNRAS, 336, 1377
Lacy, J. H., Richter, M. J., Greathouse, T. K., Jaffe, D. T., & Zhu, Q. 2002, PASP, 114, 153
Mennesson, B., et al. 2000, Proc. SPIE, 4006, 481
———. 2002, ApJ, 579, 446
Moorwood, A. F. M., & Salinari, P. 1981, A&A, 94, 299
Partridge, H., & Schwenke, D. W. 1997, J. Chem. Phys., 106, 4618
Perrin, G., Coudé du Foresto, V., Ridgway, S. T., Mennesson, B., Ruilier, C., Mariotti, J.-M., Traub, W. A., & Lacasse, M. G. 1999, A&A, 345, 221
Perrin, G., et al. 2004, A&A, in press
Quirrenbach, A., Mozurkewich, D., Armstrong, J. T., Buscher, D. F., & Hummel, C. A. 2001, BAAS, 198, 63.12
Quirrenbach, A., Mozurkewich, D., Armstrong, J. T., Johnston, K. J., Colavita, M. M., & Shao, M. 1992, A&A, 259, L19
Ridgway, S. T., Benson, J. A., Dyck, H. M., Townsley, L. K., & Hermann, R. A. 1992, AJ, 104, 2224
Tej, A., Lançon, A., & Scholz, M. 2003, A&A, 401, 347
Tuthill, P. G., et al. 1999, in ASP Conf. Ser. 194, Working on the Fringe: Optical and IR Interferometry from Ground and Space, ed. S. Unwin & R. Stachnik (San Francisco: ASP), 188
Wallace, L., & Hinkle, K. 1996, ApJS, 107, 312
Weiner, J., Hale, D. D. S., & Townes, C. H. 2003, ApJ, 588, 1064
Woitke, P., Helling, Ch., Winters, J. M., & Jeong, K. S. 1999, A&A, 348, L17
Yamamura, I., de Jong, T., & Cami, J. 1999, A&A, 348, L55
Young, J. S., et al. 1999, in IAU Symp. 191, Asymptotic Giant Branch Stars, ed. T. Le Bertre, A. Lebre, & C. Waelkens (San Francisco: ASP), 145